

1 Direct cochlear recordings show human hearing nerve 2 activity is modulated by selective attention

3 Gehmacher, Q.^{1,2*}†, Reisinger, P.^{1,2}†, Hartmann, T.^{1,2}, Keintzel, T.³, Rösch, S.⁴, Schwarz, K.⁵,
4 Weisz, N^{1,2}

5 ¹Centre for Cognitive Neuroscience, University of Salzburg, 5020 Salzburg, Austria

6 ²Department of Psychology, University of Salzburg, 5020 Salzburg, Austria

7 ³Department of Otorhinolaryngology, Klinikum Wels-Grieskirchen GmbH, 4600 Wels, Austria

8 ⁴Department of Otorhinolaryngology, Head and Neck Surgery, Paracelsus Medical University
9 Salzburg, 5020 Salzburg, Austria

10 ⁵MED-EL GmbH, 6020 Innsbruck, Austria

11 †These authors contributed equally to this work.

12 *Corresponding author: quirin.gehmacher@sbg.ac.at

13 Abstract

14 The architecture of the efferent auditory system enables prioritization of strongly overlapping
15 spatiotemporal cochlear activation patterns elicited by relevant and irrelevant inputs. So far,
16 attempts at finding such attentional modulations of cochlear activity delivered indirect insights in
17 humans or required direct recordings in animals. The extent to which spiral ganglion cells
18 forming the human hearing nerve are sensitive to selective attention remains largely unknown.
19 We investigated this question by testing the effects of attending to either the auditory or visual
20 modality on human hearing nerve activity that was directly recorded with standard commercial
21 MED-EL cochlear implants (CI) during a stimulus-free (anticipatory) cue-target interval. When
22 attending the upcoming auditory input, ongoing hearing nerve activity within the theta range (5-8
23 Hz) was enhanced. Crucially, using the broadband signal (4-25 Hz), a classifier was even able
24 to decode the attended modality from single-trial data. Follow-up analysis showed that the effect
25 was not driven by a narrow frequency in particular. Using direct cochlear recordings from deaf
26 individuals, our findings suggest that cochlear spiral ganglion cells are sensitive to top-down

27 attentional modulations. Given the putatively broad hair-cell degeneration of these individuals,
28 the effects are likely mediated by alternative efferent pathways as compared to previous studies
29 using otoacoustic emissions. Successful classification of single-trial data could additionally have
30 a significant impact on future closed-loop CI developments that incorporate real-time
31 optimization of CI parameters based on the current mental state of the user.

32 *Keywords:* auditory, cochlear implants, hearing nerve, selective attention, top-down

33 **Introduction**

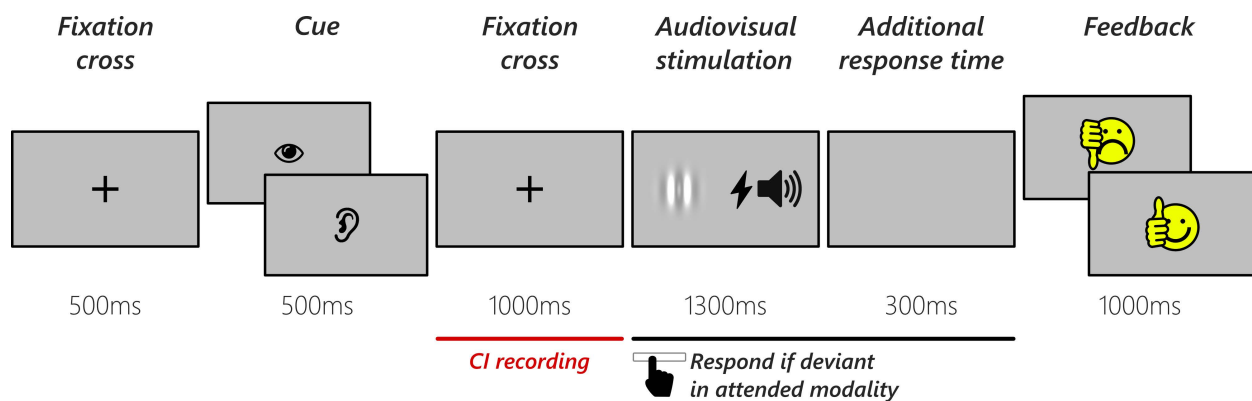
34 Attention describes a process by which sensory information can be prioritized. For all sensory
35 modalities common spatiotemporal neural activity patterns have been reported on a cortical
36 level, normally involving relevant sensory cortical regions (Frey et al., 2014; Haegens et al.,
37 2011; Händel et al., 2010; Mazaheri et al., 2014; Salo et al., 2017; Weise et al., 2016) as well as
38 higher level processing regions in frontal or parietal areas (Gazzaley & Nobre, 2012; Jackson et
39 al., 2016; Nelissen et al., 2013; Weise et al., 2016; Woolgar et al., 2015). These studies suggest
40 that selective attention is partially supported by modality-independent mechanisms. However, in
41 contrast to e.g. the visual modality, the auditory system comprises a unique complex network of
42 subcortical regions which all receive structural top-down connections originating in the auditory
43 cortex (Chandrasekaran & Kraus, 2010; Elgueda & Delano, 2020; Suga, 2008; Terreros &
44 Delano, 2015; Winer, 2006). By the most direct path, top-down information can reach the
45 cochlea via only one extra relay through the superior olivary complex (SOC). Thus, cochlear
46 activity can in principle be altered by top-down signals from the auditory cortex. However,
47 studying peripheral auditory functioning requires special recording and analysis techniques
48 (Elgueda & Delano, 2020) and has therefore been rarely investigated in this regard.

49 Noninvasively, evidence in humans comes from studies on otoacoustic emissions (OAEs),
50 sounds that are generated by outer hair cell (OHC) activity in the cochlea. Activity of OHCs are
51 modulated by a pathway from the medial olivocochlear (MOC) system that itself originates in the
52 superior olivary complex (SOC). Spiral ganglion cells making up the auditory-nerve fibers are
53 mainly innervated by connections of the lateral olivocochlear complex (LOC) respectively
54 (Elgueda & Delano, 2020; Warr & Guinan, 1979). Attentional modulations of OAEs can thus be
55 seen as a proxy for subcortical attentional modulations and have been reported for either
56 attending the left or the right ear (Giard et al., 1994) when one out of two frequencies was task

57 relevant (Maison et al., 2001) or attention had to be focused on the visual or auditory modality
58 (Dragicevic et al., 2019; Wittekindt et al., 2014). Recent work by our group (Köhler et al., in
59 press) showed that in an audiovisual attention task cochlear activity is even modulated during a
60 stimulus-free cue-target period, with enhanced theta-rhythmicity (~6 Hz) of spontaneous
61 otoacoustic activity when attending to upcoming auditory input. Yet, OAEs only deliver indirect
62 insights into the extent of the efferent auditory pathway via MOC synapses and are prone to
63 artifacts (Francis et al., 2018). Further evidence for attention modulations of cochlear activity
64 stems from direct recordings in animals. Delano et al. (2007) reported cochlear microphonic
65 (CM) increases, a measure of OHC activity, together with reductions of auditory-nerve
66 compound action potentials (CAP) in chinchillas during selective attention to visual stimuli.
67 These effects were directly recorded with chronically implanted round-window electrodes and
68 were later attributed to activation of MOC neurons, since electrical stimulation of MOC fibers
69 produced opposite effects in CAP and CM amplitudes (Elgueda et al., 2011). However, whether
70 *human* hearing nerve activity can be directly modulated via selective attention is still unknown.

71 While direct recordings are normally not feasible in humans, cochlear implants (CI) provide a
72 unique opportunity for recording hearing nerve activity. CIs restore hearing by directly applying
73 electrical stimulation to hearing nerve fibers inside the cochlea. However, the CI electrodes are
74 used to measure hearing nerve responses to short biphasic pulses to assure hearing nerve and
75 device functioning during and after surgery (Miller et al., 2008; Ramekers et al., 2014). These so
76 called electrically evoked compound action potentials (ECAPs) show a first negative N1 and a
77 second positive P1 peak (Abbas et al., 1999; He et al., 2017; Kim et al., 2010; Stypulkowski &
78 van den Honert, 1984) within the first ~0.2 ms, corresponding to wave I of the auditory
79 brainstem response (ABR; Christov et al., 2016), and can be measured with any conventional
80 CI. However, the well established effects of selective attention on a cortical (Frey et al., 2014;
81 Haegens et al., 2011; Händel et al., 2010; Mazaheri et al., 2014; Salo et al., 2017; Weise et al.,
82 2016), as well as those reported for (corticofugal) modulations of OAEs (Dragicevic et al., 2019;
83 Köhler et al., in press) on a cochlear level were reflected in slow oscillatory activity <30 Hz that
84 cannot be measured with standard short-latency ECAPs. Assuming as a working hypothesis
85 that human hearing nerve activity is modulated in a similar frequency range by selective
86 attention, our approach appended short recording windows in a stimulus-free cue-target period.
87 This technique allows for discrete sampling of that period within a single trial that can later be
88 processed like standard electroencephalographic (EEG) recordings, for example, to obtain

89 modulations of ongoing activity in relation to attention. Interestingly, CI recipients lack the
90 efferent MOC reflex that leads to cochlear dynamic compression in normal hearing
91 (Lopez-Poveda et al., 2016), suggesting damaged MOC-OHC connections after substantial
92 hair-cell degeneration. Therefore, aforementioned CI recordings during selective attention
93 should mostly reflect modulations of spiral ganglion cell activity via LOC synaptic connections.
94 Using an audiovisual crossmodal attention task adapted from Hartmann and Weisz (2019, see
95 **Figure 1**), we show that ongoing hearing nerve activity in a stimulus-free cue-target interval is
96 modulated by focused attention using standard commercial MED-EL CIs as recording devices.
97 In addition to this average condition-level effect, we show that a classifier is even able to decode
98 attended modality on a single-trial basis, which could additionally have important implications for
99 the use of conventional CIs in a closed-loop system.



100 **Figure 1.** Schematic illustration of the crossmodal attention task. Each trial started with a fixation cross,
101 followed by a cue indicating either to attend the visual or auditory domain. A second fixation cross
102 appeared and an auditory and visual stimulus were presented afterwards. When the stimulus in the
103 attended modality was deviant (visual: gabor patch tilt, auditory: oddball sound), participants had to
104 respond by pressing the spacebar. The additional response time accounted for trials where the gabor
105 patch tilted towards the end of the stimulation. At the end of each trial, feedback was given in the form of
106 a smiley face. The red line denotes the time window where hearing nerve activity was recorded via the CI.

107 Results

108 Sixteen CI users performed a crossmodal attention task (similar to Hartmann & Weisz, 2019)
109 where attention had to be focused on an upcoming auditory or visual stimulus (see **Figure 1**).
110 Hearing nerve activity was recorded directly via one of their standard CI electrodes in the
111 stimulus-free cue-target interval. We calculated the power spectral density of the signal and

112 compared the two conditions (attend auditory vs. visual) in the theta and alpha band.
113 Afterwards, a classifier was utilized to decode the attended modality on a single-trial basis using
114 the broadband signal and frequency bands typically associated with selective attention (theta,
115 alpha, beta).

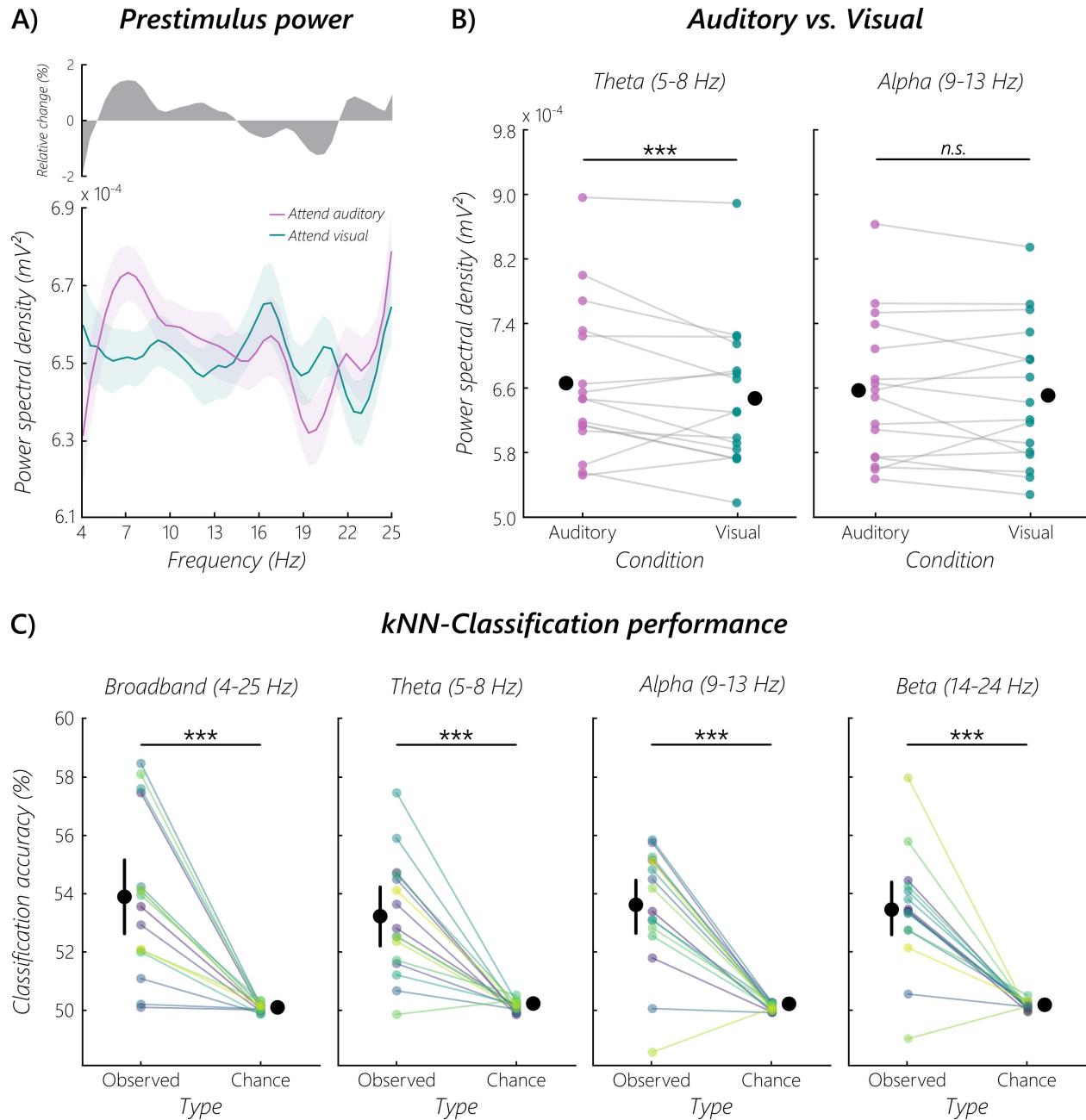
116 *Behavioral results*

117 Participants gave a correct response in 96% ($SD = 2.7\%$) of all trials. The number of correct
118 trials did not differ significantly between the two conditions, according to a dependent sample
119 t-test (auditory: $M = 245$ ($SD = 9.8$); visual: $M = 242$ ($SD = 8.8$); $t(15) = 1.32$, $p = 0.21$, $d = 0.33$).
120 When there was an oddball in the cued domain, a correct response was given in 75% ($SD =$
121 19.0%) of the trials. In the auditory condition, the percentage of correct oddball trials was 72%
122 ($SD = 30.8\%$) and in the visual condition 78% ($SD = 14.2\%$). Overall, the behavioral findings
123 suggested that participants performed the task in a compliant manner.

124 *Human hearing nerve activity is modulated by selective attention*

125 In a first analysis step, we calculated the broadband PSD from 4-25 Hz, separately for each
126 condition (attend auditory/attend visual). The resulting power spectra (see **Figure 2A**) by
127 themselves showed no clear peaks, however the grand average condition contrast spectrum
128 indicates differences that are mainly centered in distinct frequency ranges. Based on previous
129 OAE and M/EEG work (Köhler et al., in press; Mazaheri et al., 2014), we statistically compared
130 the two conditions in the theta (averaged between 5-8 Hz) and alpha frequency band (averaged
131 between 9-13 Hz; **Figure 2B**). A cluster-based permutation test in the theta frequency band
132 showed that prestimulus power is higher when attending the auditory domain ($p = 10.00e^{-05}$, $d =$
133 0.49). No cluster was found in the alpha frequency band ($p = 1.00$, $d = 0.20$). Given the
134 distribution of the individual average power in both FOI, a rather high interindividual variability
135 can be seen.

136 The results so far showed that selective attention modulates directly recorded cochlear activity,
137 with the effect being in particular pronounced in the theta frequency range: attending to an
138 upcoming auditory stimulus resulted in higher power recorded from the CI electrode.



139 **Figure 2. Prestimulus power modulations and decoding of selective attention.** (A) Grand average
 140 prestimulus power spectra from 4-25 Hz when attending the auditory or visual domain. The top panel
 141 indicates the relative change between the auditory and visual domain. The shaded areas in the bottom
 142 panel represent the standard error of the mean for within-subjects designs (O'Brien & Cousineau, 2014).
 143 (B) Average prestimulus power in the theta and alpha band, separated by the two conditions. Black dots
 144 indicate the group mean for the respective condition. A cluster-based permutation test in the averaged
 145 theta FOI resulted in a statistically significant difference when testing the hypothesis that performance is
 146 higher when attending the auditory domain ($p = 10.00e^{-05}$, $d = 0.49$). No cluster was found in the alpha
 147 band ($p = 1.00$, $d = 0.20$). The asterisks indicate a statistically significant difference (n.s. = not significant).
 148 (C) A kNN-Classifier was used to decode attended modality from single-trial prestimulus power spectra.
 149 Resulting *Observed* accuracies were contrasted with respective *Chance* levels of a random permutation

150 test for all FOI. Contrasts revealed significant ($p < 0.001$) decoding performance throughout spectra with
151 fairly similar effects (broadband: $t(15) = 5.60$, $p = 2.60e^{-05}$, $d = 1.96$; theta: $t(15) = 5.83$, $p = 1.70e^{-05}$, $d =$
152 2.11; alpha: $t(15) = 6.78$, $p = 3.00e^{-06}$, $d = 2.34$; beta: $t(15) = 6.40$, $p = 6.00e^{-06}$, $d = 2.33$) on a group level
153 (represented by black dots; error bars = 95% CI). However, on a single-subject level the attention effect
154 was most pronounced for individually specific FOI, resulting in significant above chance decoding for 12
155 out of 16 subjects. Every subject is represented by the same color in all four FOI columns.

156 *Attended modality can be decoded from single-trial CI recordings*

157 We used prestimulus power spectra for a kNN-Classifer to show that attention modulation of
158 ongoing hearing nerve activity in humans is even reflected in single-trial CI recordings. To
159 ensure that the classifier was able to differentiate hearing nerve activity when attending the
160 auditory compared to the visual domain in general, we calculated a t-test between *Observed*
161 classification accuracies and respective *Chance* levels of broadband power spectra, showing
162 that this attention effect was decodable significantly above chance ($t(15) = 5.60$, $p = 2.60e^{-05}$, $d =$
163 1.96; **Figure 2C**). Given the significant difference over a broad frequency range, we were further
164 interested in whether this attention effect was driven by one of the FOI usually connected with
165 selective attention in OAE and M/EEG studies. We therefore calculated a two-factor repeated
166 measures ANOVA to compare the effect of selective attention on kNN-Classification accuracy
167 for different FOI (broadband, theta, alpha, beta) and Types (*Observed*, *Chance*). Results show
168 no significant effect of FOI ($F(3, 45) = 0.37$, $p = 0.78$, $\eta_p^2 = 0.02$), yet show a significant effect for
169 *Observed* vs. *Chance* accuracies ($F(1, 15) = 136.55$, $p = 6.21e^{-09}$, $\eta_p^2 = 0.90$), with higher
170 accuracies for *Observed* ($M = 0.53$) than *Chance* ($M = 0.50$) levels. No FOI x Type interaction
171 on decoding results was found ($F(3, 45) = 0.36$, $p = 0.78$, $\eta_p^2 = 0.02$). As a main effect of Type
172 and no interaction of FOI x Type indicated that selective attention can be decoded from all FOI
173 separately, in addition we computed three t-tests for theta, alpha, and beta bands contrasting
174 respective *Observed* and *Chance* levels. For all three FOI a significant difference was found for
175 selective attention decoding (theta: $t(15) = 5.83$, $p = 1.70e^{-05}$, $d = 2.11$; alpha: $t(15) = 6.78$, $p =$
176 $3.00e^{-06}$, $d = 2.34$; beta: $t(15) = 6.40$, $p = 6.00e^{-06}$, $d = 2.33$; **Figure 2C**). Additionally, random
177 permutation tests of kNN classification within all four different FOI gave insights into
178 single-subject decoding performance across the different frequency spectra. Independent of
179 FOI, an overall number of 12 subjects (i.e. 75% of the sample) showed significant ($p < 0.05$)
180 above chance decoding of focused attention during the stimulus-free cue-target interval.

181 Discussion

182 The efferent auditory system comprises a complex arrangement of subcortical and peripheral
183 pathways where - uniquely among the senses - the cochlear activity can be altered by top-down
184 signals from the auditory cortex via the SOC (Chandrasekaran & Kraus, 2010; Elgueda &
185 Delano, 2020; Suga, 2008; Terreros & Delano, 2015; Winer, 2006). Profound evidence supports
186 the notion of altered oscillatory neural activity by selective attention on a cortical level (Frey et
187 al., 2014; Haegens et al., 2011; Händel et al., 2010; Mazaheri et al., 2014; Salo et al., 2017;
188 Weise et al., 2016), prioritizing attended over unattended events in the environment which is
189 predominantly reflected in modulations within the alpha band (~9-13 Hz; Frey et al., 2014;
190 Sauseng et al., 2005; for a review see Foxe & Snyder, 2011; notably also Antonov et al., 2020
191 that challenges current views). While such changes have also been reported for the auditory
192 cortex (Weisz et al., 2011), much less is known for subcortical structures along the efferent
193 pathway. This is in particular the case when it comes to the *human* cochlea as special recording
194 and analysis techniques are required (Elgueda & Delano, 2020). So far, investigating attentional
195 modulation of cochlear activity in humans had to rely on indirect recordings of OAEs; a
196 noninvasive approach for measuring OHC activity that receives modulatory signals from the
197 SOC through its medial neurons (MOC). Recent evidence suggests slow modulations of
198 cochlear activity when attention had to be focused on the auditory modality. Dragicevic et al.
199 (2019) were the first ones to establish attention-related modulations of distortion product OAE
200 (DPOAE) activity in a low (<10 Hz) frequency range. Going beyond these stimulus-evoked
201 changes, even when no auditory stimulus is presented, cochlear activity is enhanced in an
202 analogous frequency range as shown by Köhler et al. (in press). These striking results provide
203 substantial evidence for a notable role of selective attention at the very first stages of sound
204 processing in the human auditory system. However, in addition to an indirect measurement
205 approach that is prone to artifacts (Francis et al., 2018), studying OAEs cannot address direct
206 modulation of hearing nerve activity since spiral ganglion cells are efferently innervated by a
207 separate pathway. To our knowledge, this attentional modulation via the LOC remains
208 completely unknown as direct recordings of hearing nerve activity are normally not feasible in
209 humans. Given the damage to OHCs and their connections to the MOC in CI recipients
210 (Lopez-Poveda et al., 2016) potential alterations of respective hearing nerve activity in a
211 selective attention paradigm should largely reflect top-down signals from the LOC. Our results,
212 contrasting direct cochlear recordings during auditory and visual attention, show that ongoing

213 hearing nerve activity is top-down modulated, putatively suggesting a role of the LOC pathway
214 in selective attention.

215 While cortical and OAE-based measures suggest attention-related effects in distinct frequency
216 bands (Köhler et al., in press; Mazaheri et al., 2014), our results are mixed in this respect. The
217 broadband frequency analysis of the prestimulus interval showed no clear peaks (**Figure 2A**).
218 This, however, may also be the result of low signal-to-noise ratios (SNRs), as commercial CIs
219 are so far not optimized to do these kinds of continuous electrophysiological recordings. Indeed
220 a grand average of the condition differences points to maximal effects in a frequency range
221 overlapping with the one reported by Köhler et al. (in press). When analyzing the prestimulus
222 power spectra in two FOI (theta and alpha), we found a selective attention effect in theta
223 resulting in enhanced power while attending to the auditory modality (**Figure 2B**). This result
224 corroborates our previous finding using a similar paradigm, where ongoing OAEs in the theta
225 band (~6 Hz) were enhanced while attending an upcoming auditory stimulus (Köhler et al., in
226 press). We found no selective attention effect in the alpha band in concordance with
227 aforementioned studies of otoacoustic activity. It is therefore possible that this frequency band
228 does not play a central role in selective attention at the peripheral level. Further studies with an
229 optimized recording setup will be necessary to address this issue.

230 Building upon conventional analyses of condition-level fast Fourier transform (FFT) averages,
231 we decided to use single-trial frequency spectra to classify anticipatory attentional focus during
232 the stimulus-free cue-target period. With this approach we aimed to get more detailed insight
233 into fine-grained differences between attentional states coded within modulations of direct
234 cochlear recordings that could be missed by condition-level averaging approaches and indirect
235 OAE measurements. Strikingly, classification of the broadband signal (4-25 Hz) revealed
236 significantly improved differentiation of attended modality compared to the average
237 condition-level effect of the FFT results (**Figure 2C**). There seems to be sufficient top-down
238 modality specific information entailed in single-channel CI recordings to ensure above chance
239 classification performance without even specifying a particular attention-related frequency band
240 - a clear improvement to the standard FFT approach. As a matter of fact, follow-up analysis
241 showed that the performance was not driven by one of three FOI (theta, alpha, beta) usually
242 associated with selective attention, but instead it revealed that the contribution of each of these
243 frequency bands to broadband classification was fairly similar. However, the decoding approach
244 allowed for additional insight into single-subject classification performance and showed high

245 interindividual variability in terms of an optimal spectral frequency band. It remains to be
246 determined whether this effect is driven by local idiosyncrasies at the peripheral level (e.g.
247 synaptic connections between LOC and spiral ganglion cells) or even involves particular activity
248 patterns at higher hierarchical levels. Independent of the precise origins of our effects observed
249 at the hearing nerve, the decoding results open up avenues to future developments towards
250 closed-loop CIs that incorporate mental states of the recipient reflected in cochlear activity into
251 adaptive stimulation in real time. Attempts so far with standard modern CIs required exhaustive
252 recording and analysis sessions and indicated additional hard- and software modifications (Mc
253 Laughlin et al., 2012) in order to extract meaningful neuronal activity with additional
254 extracochlear (i.e. EEG) electrodes, especially for real time applications. In the present study,
255 we used standard commercial MED-EL CIs to record ongoing activity directly at the hearing
256 nerve during a stimulus-free anticipatory cue-target interval without additional electrodes or
257 implantations. As we show, a classifier could use the frequency information of this signal to
258 anticipate the attentional state of the recipient. Future research will need to address which
259 cognitive states can be decoded directly at the hearing nerve and how this information could be
260 exploited in a closed-loop CI setup.

261 This study shows that individuals with a CI form a model population to deepen our
262 understanding of how cognition can lever the efferent auditory system to modulate auditory
263 input at the earliest stages of processing. In the present study we focused on stimulation-free
264 anticipatory cue-target periods using a popular experimental setup in cognitive neuroscience
265 (Hartmann & Weisz, 2019; Köhler et al., in press; Posner, 1980; Wittekindt et al., 2014). The
266 extent to which the identified top-down modulations also play a role in more complex
267 environments with natural speech, for example in attending one of multiple speakers at a
268 “cocktail-party”, should be addressed in further studies and could add valuable information to an
269 ongoing debate on speech processing in such scenarios. As CI recipients show highly varying
270 listening success in multitalker situations (Loizou et al., 2009), their ability to (re-)engage the
271 path from the LOC to auditory-nerve fibers in selective processing could play a key role in
272 coping post-operatively with those situations. Future studies could combine our direct cochlear
273 recording approach with EEG-based measurements of cortical modulations during selective
274 attention. However, so far technical restrictions by the device itself (Abbas et al., 2017;
275 Campbell et al., 2015; Tejani et al., 2019) and superimposing artifacts that would be caused by
276 the stimulation with complex sounds like speech don’t allow researchers to use CI electrodes for

277 simultaneous stimulation and recording of hearing nerve activity and needed to be optimized for
278 such continuous applications in future developments. Nonetheless, our approach shows that
279 ongoing hearing nerve activity contains relevant and, crucially, classifiable information about
280 current attentional status that could be used to adapt the CI's processing strategy, resulting in
281 less fatigue and higher intelligibility during challenging listening situations.

282 In summary, to the best of our knowledge our study is the first to investigate attentional effects
283 on activity recorded directly from the hearing nerve in humans. We confirm and extend previous
284 indirect measurements, suggesting attentional modulations in the theta frequency range.
285 Importantly, we also show that selective attention can be decoded above chance at a single-trial
286 and even individual level. Previous reports on attentional modulations of cochlear activity relied
287 on OAEs, which are driven by the MOC pathway. Our results strongly suggest that the LOC
288 pathway can also be exploited in a top-down down fashion to affect spiral ganglion cells directly.

289 **Materials and Methods**

290 *Participants*

291 21 right-handed CI users (4 females, $M_{\text{age}} = 57.5$, $SD_{\text{age}} = 11.9$) participated in the study, all with
292 a minimum CI experience of six months. Participants were recruited via the ENT departments of
293 the hospitals in Salzburg ($n = 10$) and Wels-Grieskirchen ($n = 11$). Three participants were
294 excluded because of a too weak contact between transmitting CI coil and receiver that was
295 required for the study. One participant showed no N1 in recorded ECAPs, which could indicate a
296 measurement problem and was therefore excluded. One participant quit during the session due
297 to concentration problems. This led to a final sample size of 16 participants (3 females, $M_{\text{age}} =$
298 53.8 , $SD_{\text{age}} = 12.0$; see Table S1 for further details). All participants reported no previous
299 neurological or psychiatric disorders, and reported normal or corrected-to-normal vision. All
300 participants signed an informed consent and were reimbursed with 10 Euro per hour. The
301 experimental protocol was approved by the ethics committee of the University of Salzburg and
302 was carried out in accordance with the Declaration of Helsinki.

303 *Stimuli and Procedure*

304 The experimental procedure was implemented in MATLAB 8.6 (The MathWorks Inc., Natick,
305 Massachusetts, USA) using custom scripts. Presentation of visual stimuli and response

306 collection was achieved with a previous version (th_ptb; https://gitlab.com/thht/th_ptb) of the
307 Objective Psychophysics Toolbox (o_ptb; Hartmann & Weisz, 2020), which adds an additional
308 class-based abstraction layer in addition to the Psychophysics Toolbox (Version 3.0.14;
309 Brainard, 1997; Kleiner et al., 2007; Pelli, 1997). Cochlear stimulation as well as recording was
310 performed via the MAX Programming Interface, a device which is part of the clinical standard
311 setup that enables control of the implant, together with the Research Interface Box 2
312 Dynamic-link library (RIB2 DLL provided by the University of Innsbruck, Innsbruck, AT; Litovsky
313 et al., 2017). To ensure accurate stimulus presentation and triggering, timings were measured
314 with the Black Box ToolKit v2 (The Black Box ToolKit Ltd., Sheffield, UK).

315 Participants were seated in front of a computer screen and were asked to remove their CI
316 processor and coil to replace it with a coil connected to the MAX Programming Interface. For
317 bilateral CI users, the side with the better subjective hearing performance and/or longer
318 implantation date was used (see Table S1). Primarily the CI coil model MAX Coil was used, but
319 if the magnet was too weak to ensure a stable connection, the CI coil model MAX Coil S was
320 used. As a first step, the individual electrical hearing threshold was determined with a standard
321 tone with a stimulation frequency of 100 Hz and a duration of 300 ms. To ensure that the
322 auditory stimulation was at a comfortable level during the experiment, the individual maximum
323 loudness was determined, for the standard and an oddball tone respectively. An oddball tone
324 with the maximum possible stimulation frequency of 9990 Hz (based on the used phase
325 duration of 30 μ s per phase for sequential biphasic pulses) and a duration of 300 ms was used.
326 The described routines were implemented using custom scripts and the Palamedes Toolbox
327 (Prins & Kingdom, 2018). Afterwards, as a functionality check of the measurement setup,
328 ECAPs were recorded (for further details, see Methods S1; Bahmer et al., 2010). For the
329 crossmodal attentional task described later, it was necessary that two stimulation frequencies
330 could be distinguished. Because of interindividual differences when hearing with a CI, it was
331 necessary to adjust these stimulation frequencies for every participant. Participants were asked,
332 after hearing a standard and oddball tone, if the first or the second tone had a higher stimulation
333 frequency. The standard tone had a stimulation frequency of 100 Hz and a duration of 300 ms.
334 The initial stimulation frequency of the oddball tone (also with a duration of 300 ms) was
335 determined by the results of the aforementioned maximum loudness procedure. This procedure
336 was carried out using a Bayesian active sampling protocol to estimate the model parameters of
337 the psychometric function (Kontsevich & Tyler, 1999; Sanchez et al., 2016) and was

338 implemented with the VBA Toolbox (Daunizeau et al., 2014). To define the individual oddball
339 stimulation frequency for the subsequent crossmodal attention task, the algorithm searched for
340 the optimal difference in logarithmic steps from 1 to 9890 Hz and this value was subsequently
341 added to the standard stimulation frequency. Six participants heard no clear difference and it
342 was necessary to adjust the oddball stimulation frequency manually, with values between 114
343 and 600 Hz.

344 The actual experiment was carried out as a crossmodal attention task (see **Figure 1**; similar to
345 Hartmann & Weisz, 2019) in six blocks, with 85 trials per block. Each trial started with a 500 ms
346 fixation cross, followed by a cue that indicated either to attend the auditory or the visual
347 modality. Every block had 43 auditory and 42 visual cues. The cue was a picture of an eye or
348 ear, presented for 500 ms. A second fixation cross appeared for 1000 ms and the audiovisual
349 stimulation started afterwards. The auditory stimulation consisted of a 300 ms tone with a
350 stimulation frequency of 100 Hz and was directly presented via the CI coil. The visual
351 stimulation was a vertically oriented gabor patch (spatial frequency: 0.01 cycles/pixel, sigma: 60
352 pixels, phase: 90°), presented for 1300 ms in the center of the screen. In every block, 8 trials
353 were randomly chosen as visual oddball trials. Independently, another 8 trials were chosen to be
354 auditory oddball trials. Therefore it was possible that a trial was a visual and auditory oddball
355 trial simultaneously. In visual oddball trials, the gabor patch tilted 10° to the left, with a random
356 onset. In auditory oddball trials, a 300 ms tone with the individual oddball stimulation frequency
357 was presented. Participants had to press the spacebar if the current trial had an oddball in the
358 cued domain. To account for trials where the visual oddball onset was towards the end of the
359 stimulation, an additional response time of 300 ms was provided. After each trial, feedback in
360 the form of a smiley face displayed for 1000 ms, indicated if the response was correct or not. To
361 ensure correct understanding of and response during the task, participants completed one block
362 as a practice run before the actual experiment. The total duration of the experiment was about
363 90 minutes including breaks and preparation.

364 *Recording of hearing nerve activity*

365 We exploit the ability of CIs to record electrical activity from the cochlea in short time windows,
366 but in contrast to previous approaches (Abbas et al., 2017; Mc Laughlin et al., 2012), in a
367 stimulus-free cue-target period. Using a custom developed MATLAB toolbox to abstract MAX
368 Programming Interface commands, we recorded hearing nerve activity via the CI electrode (for

369 bilateral CI users, see Table S1 which side was used). In every participant, the first (i.e. most
370 apical) electrode was used for the recordings. Each recording window was 1.7 ms long, followed
371 by a 13.68 ms reset period resulting in a sampling frequency of 65 Hz (1.7 ms recording + 13.68
372 ms reset time). The technical specifics of the measurement system added a random offset to
373 each of the recordings (Gaussian noise, $SD = 0.4$ mV). Because of the USB connection
374 between the computer and the MAX Programming Interface, the start of the first recording
375 window had a jitter of 27 ms, but the system sent a highly precise trigger when it started. Due to
376 technical limitations, it was not possible to record and stimulate simultaneously. We performed
377 recordings in the 1000 ms prestimulus window (see red line in **Figure 1**).

378 *Data preprocessing*

379 The raw data was analyzed in MATLAB 9.8 (The MathWorks, Natick, Massachusetts, USA).
380 Due to filter artifacts (using the standard filter from the used RIB2 package), the first 100
381 samples (= 0.083 ms) from every recording window were discarded. Afterwards, the recording
382 was averaged and treated as one sample point. By repeating these steps for every window and
383 concatenating the single samples, a recording length of 1 second with a sampling frequency of
384 65 Hz was reached. The data was further preprocessed with the FieldTrip toolbox (revision
385 ea6897bb7; Oostenveld et al., 2010) and a bandpass filter between 4 and 25 Hz was applied
386 (hamming-windowed sinc FIR filter, onepass-zerophase, order: 424, transition width: 0.5 Hz).
387 For one participant, 15 trials had to be rejected because the CI coil fell off during the last trials of
388 one block. Only trials with a correct response were analyzed, which were on average 488 trials
389 ($SD = 15.8$). The number of correct trials was not significantly different between the two
390 conditions (see Behavioral results).

391 *Frequency analysis*

392 Next, data was demeaned, detrended and power spectral density (PSD) from 4 to 25 Hz was
393 computed on the whole 1000 ms prestimulus window ('mtmfft' implementation in FieldTrip with a
394 Hann window) separately for the two conditions. For **Figure 2A**, no bandpass filter was applied,
395 condition-specific power spectra were smoothed (five-point moving average), grand-averaged,
396 and corrected error bars for within-subjects designs were calculated (O'Brien & Cousineau,
397 2014).

398 We defined two frequency bands of interest (FOI), theta (5-8 Hz) and alpha (9-13 Hz). Theta
399 was selected because of previous work on OAEs that showed attentional modulations in this
400 FOI (Dragicevic et al., 2019; Köhler et al., in press). On a cortical level, previous work showed
401 that auditory alpha activity reflects attentional processes (Frey et al., 2014; Mazaheri et al.,
402 2014; Müller & Weisz, 2012; Weise et al., 2016; Weisz et al., 2014; for a review see Weisz et
403 al., 2011). Therefore, we decided to analyze this FOI at the cochlear level.

404 To test the hypothesis that power was higher when the auditory domain was attended, statistical
405 testing of PSD was performed with a cluster-based permutation test (dependent samples t-test,
406 10000 randomizations, one-tailed; Maris & Oostenveld, 2007). We averaged the theta and alpha
407 FOI and tested them separately.

408 *Decoding analysis*

409 For decoding of attended modality on a single-trial basis, we performed k-nearest neighbors
410 (kNN) classification of single-trial power spectra using scikit-learn (Version 0.23.1 running on
411 Python 3.7.7; Pedregosa et al., 2011) separately for a broadband signal (4-25 Hz) followed by
412 standard frequency bands associated with selective attention (theta: 5-8 Hz, alpha: 9-13 Hz,
413 beta: 14-24 Hz). We decided to use the kNN classification approach as data was recorded from
414 a single CI channel over a one second period resulting in low numbers of features (i.e.
415 frequency points per band), a classification problem usually solved better by a kNN approach
416 (Eisa et al., 2018). At first, a subject's data was standardized to unit variance and zero mean.
417 For the classification process of each subject, the best number of neighbors was determined by
418 searching the hyper-parameter space for the best cross-validation (CV) score of a kNN model
419 using the implemented *GridSearchCV* function with a 2-fold CV on shuffled class samples
420 (*StratifiedKfold(shuffle=True)*) that was fit to the data for every FOI. Our decision for a 2-fold CV
421 was based on recommendations in case of low sample / effect size data (Jamalabadi et al.,
422 2016). The numbers of neighbors to use during the gridsearch were defined as ranging from
423 one to 10% of trials in the dataset in odd numbers (1, trials/10, stepsize=2) to avoid the conflict
424 of even neighbors in a two-class problem (attend auditory vs. visual). Given the novel approach,
425 we could not exclude that the classifier would pick up on a few outlying data points. In order to
426 address this issue explicitly, the classifier was tested on the same noisy data, albeit with
427 randomly shuffled condition labels. Samples were thus classified and tested for significance with

428 the best scoring number of neighbors in a 1000 random permutation test and the 2-fold CV
429 procedure.

430 The resulting *Observed* and *Chance* accuracy values (where chance level was calculated as the
431 mean accuracy of the 1000 random permutation scores) for every FOI were then statistically
432 tested using pingouin (Version 0.3.8 running on Python 3.7.7; Vallat, 2018). In a first step, to test
433 whether hearing nerve modulation was generally reflected within classification results,
434 broadband values (*Observed* vs. *Chance*) were compared using a one-sided t-test. Then,
435 classification results of all four FOI were compared in a two-factor repeated measures ANOVA
436 with the factors *FOI* (broadband, theta, alpha, beta) and *Type* (*Observed* vs. *Chance*) to check
437 whether the attention effect was driven by one of the predefined FOI. Finally, theta, alpha, and
438 beta bands were also tested for significant differences during focused attention computing three
439 one-sided t-tests with respective values (*Observed* vs. *Chance*).

440 **Acknowledgments**

441 The authors would like to thank Agnes Koller and Lisa Niederwanger for their help in recruiting
442 participants. Quirin Gehmacher and Patrick Reisinger are supported by the Austrian Research
443 Promotion Agency (FFG; BRIDGE 1 project "SmartCIs"; 871232) and the Austrian Science
444 Fund (FWF; Doctoral College "Imaging the Mind"; W 1233-B).

445 **Author Contributions**

446 Q.G. and P.R. collected and analyzed data, generated the figures, and wrote the manuscript.
447 T.H. designed the experiment, collected and analyzed data, developed analysis methods, and
448 edited the manuscript. T.K. and S.R. recruited participants and consulted on the clinical aspects.
449 K.S. developed analysis methods, provided input on data analysis, and edited the manuscript.
450 N.W. acquired the funding, supervised the project, and edited the manuscript.

451 **Declaration of Interests**

452 K.S. is an employee of MED-EL GmbH. All other authors declare no competing interests.

453 **References**

- 454 Abbas, P. J., Brown, C. J., Shallop, J. K., Firszt, J. B., Hughes, M. L., Hong, S. H., & Staller, S.
455 J. (1999). Summary of Results Using the Nucleus CI24M Implant to Record the
456 Electrically Evoked Compound Action Potential. *Ear and Hearing*, 20(1), 45–59.
457 <https://doi.org/10.1097/00003446-199902000-00005>
- 458 Abbas, P. J., Tejani, V. D., Scheperle, R. A., & Brown, C. J. (2017). Using Neural Response
459 Telemetry to Monitor Physiological Responses to Acoustic Stimulation in Hybrid
460 Cochlear Implant Users. *Ear and Hearing*, 38(4), 409.
461 <https://doi.org/10.1097/AUD.0000000000000400>
- 462 Antonov, P. A., Chakravarthi, R., & Andersen, S. K. (2020). Too little, too late, and in the wrong
463 place: Alpha band activity does not reflect an active mechanism of selective attention.
464 *NeuroImage*, 219, 117006. <https://doi.org/10.1016/j.neuroimage.2020.117006>
- 465 Bahmer, A., Peter, O., & Baumann, U. (2010). Recording and analysis of electrically evoked
466 compound action potentials (ECAPs) with MED-EL cochlear implants and different
467 artifact reduction strategies in Matlab. *Journal of Neuroscience Methods*, 191(1), 66–74.
468 <https://doi.org/10.1016/j.jneumeth.2010.06.008>
- 469 Brainard, D. H. (1997). The Psychophysics Toolbox. *Spatial Vision*, 10(4), 433–436.
470 <https://doi.org/10.1163/156856897X00357>
- 471 Campbell, L., Kaicer, A., Briggs, R., & O'Leary, S. (2015). Cochlear Response Telemetry:
472 Intracochlear Electrocochleography via Cochlear Implant Neural Response Telemetry
473 Pilot Study Results. *Otology & Neurotology*, 36(3), 399.
474 <https://doi.org/10.1097/MAO.0000000000000678>
- 475 Chandrasekaran, B., & Kraus, N. (2010). The scalp-recorded brainstem response to speech:
476 Neural origins and plasticity. *Psychophysiology*, 47(2), 236–246.

- 477 <https://doi.org/10.1111/j.1469-8986.2009.00928.x>
- 478 Christov, F., Munder, P., Berg, L., Bagus, H., Lang, S., & Arweiler-Harbeck, D. (2016). ECAP
479 analysis in cochlear implant patients as a function of patient's age and electrode-design.
480 *European Annals of Otorhinolaryngology, Head and Neck Diseases*, 133, S1–S3.
481 <https://doi.org/10.1016/j.anorl.2016.04.015>
- 482 Daunizeau, J., Adam, V., & Rigoux, L. (2014). VBA: A Probabilistic Treatment of Nonlinear
483 Models for Neurobiological and Behavioural Data. *PLOS Computational Biology*, 10(1),
484 e1003441. <https://doi.org/10.1371/journal.pcbi.1003441>
- 485 Delano, P. H., Elgueda, D., Hamame, C. M., & Robles, L. (2007). Selective Attention to Visual
486 Stimuli Reduces Cochlear Sensitivity in Chinchillas. *Journal of Neuroscience*, 27(15),
487 4146–4153. <https://doi.org/10.1523/JNEUROSCI.3702-06.2007>
- 488 Dragicevic, C. D., Marcenaro, B., Navarrete, M., Robles, L., & Delano, P. H. (2019). Oscillatory
489 infrasonic modulation of the cochlear amplifier by selective attention. *PLOS ONE*, 14(1),
490 e0208939. <https://doi.org/10.1371/journal.pone.0208939>
- 491 Eisa, D. A., Taloba, A. I., & Ismail, S. S. I. (2018). A Comparative Study on using Principle
492 Component Analysis with different Text Classifiers. *International Journal of Computer
493 Applications*, 180(31), 1–6. <https://doi.org/10.5120/ijca2018916800>
- 494 Elgueda, D., & Delano, P. H. (2020). Corticofugal modulation of audition. *Current Opinion in
495 Physiology*, 18, 73–78. <https://doi.org/10.1016/j.cophys.2020.08.016>
- 496 Elgueda, D., Delano, P. H., & Robles, L. (2011). Effects of Electrical Stimulation of Olivocochlear
497 Fibers in Cochlear Potentials in the Chinchilla. *Journal of the Association for Research in
498 Otolaryngology*, 12(3), 317–327. <https://doi.org/10.1007/s10162-011-0260-9>
- 499 Foxe, J. J., & Snyder, A. C. (2011). The Role of Alpha-Band Brain Oscillations as a Sensory
500 Suppression Mechanism during Selective Attention. *Frontiers in Psychology*, 2.

- 501 <https://doi.org/10.3389/fpsyg.2011.00154>
- 502 Francis, N. A., Zhao, W., & Guinan Jr., J. J. (2018). Auditory Attention Reduced Ear-Canal
503 Noise in Humans by Reducing Subject Motion, Not by Medial Olivocochlear Efferent
504 Inhibition: Implications for Measuring Otoacoustic Emissions During a Behavioral Task.
505 *Frontiers in Systems Neuroscience*, 12. <https://doi.org/10.3389/fnsys.2018.00042>
- 506 Frey, J. N., Mainy, N., Lachaux, J.-P., Müller, N., Bertrand, O., & Weisz, N. (2014). Selective
507 Modulation of Auditory Cortical Alpha Activity in an Audiovisual Spatial Attention Task.
508 *Journal of Neuroscience*, 34(19), 6634–6639.
509 <https://doi.org/10.1523/JNEUROSCI.4813-13.2014>
- 510 Gazzaley, A., & Nobre, A. C. (2012). Top-down modulation: Bridging selective attention and
511 working memory. *Trends in Cognitive Sciences*, 16(2), 129–135.
512 <https://doi.org/10.1016/j.tics.2011.11.014>
- 513 Giard, M.-H., Collet, L., Bouchet, P., & Pernier, J. (1994). Auditory selective attention in the
514 human cochlea. *Brain Research*, 633(1), 353–356.
515 [https://doi.org/10.1016/0006-8993\(94\)91561-X](https://doi.org/10.1016/0006-8993(94)91561-X)
- 516 Haegens, S., Nácher, V., Luna, R., Romo, R., & Jensen, O. (2011). α -Oscillations in the monkey
517 sensorimotor network influence discrimination performance by rhythmical inhibition of
518 neuronal spiking. *Proceedings of the National Academy of Sciences*, 108(48),
519 19377–19382. <https://doi.org/10.1073/pnas.1117190108>
- 520 Händel, B. F., Haarmeier, T., & Jensen, O. (2010). Alpha Oscillations Correlate with the
521 Successful Inhibition of Unattended Stimuli. *Journal of Cognitive Neuroscience*, 23(9),
522 2494–2502. <https://doi.org/10.1162/jocn.2010.21557>
- 523 Hartmann, T., & Weisz, N. (2019). Auditory cortical generators of the Frequency Following
524 Response are modulated by intermodal attention. *NeuroImage*, 203, 116185.

- 525 <https://doi.org/10.1016/j.neuroimage.2019.116185>
- 526 Hartmann, T., & Weisz, N. (2020). An introduction to the Objective Psychophysics Toolbox.
527 *Frontiers in Psychology, 11*. <https://doi.org/10.3389/fpsyg.2020.585437>
- 528 He, S., Teagle, H. F. B., & Buchman, C. A. (2017). The electrically evoked compound action
529 potential: From laboratory to clinic. *Frontiers in Neuroscience, 11*.
530 <https://doi.org/10.3389/fnins.2017.00339>
- 531 Jackson, J., Rich, A. N., Williams, M. A., & Woolgar, A. (2016). Feature-selective Attention in
532 Frontoparietal Cortex: Multivoxel Codes Adjust to Prioritize Task-relevant Information.
533 *Journal of Cognitive Neuroscience, 29*(2), 310–321.
534 https://doi.org/10.1162/jocn_a_01039
- 535 Jamalabadi, H., Alizadeh, S., Schönauer, M., Leibold, C., & Gais, S. (2016). Classification
536 based hypothesis testing in neuroscience: Below-chance level classification rates and
537 overlooked statistical properties of linear parametric classifiers. *Human Brain Mapping,*
538 *37*(5), 1842–1855. <https://doi.org/10.1002/hbm.23140>
- 539 Kim, J.-R., Abbas, P. J., Brown, C. J., Etler, C. P., O'Brien, S., & Kim, L.-S. (2010). The
540 Relationship Between Electrically Evoked Compound Action Potential and Speech
541 Perception: A Study in Cochlear Implant Users With Short Electrode Array. *Otology &*
542 *Neurotology, 31*(7), 1041–1048. <https://doi.org/10.1097/MAO.0b013e3181ec1d92>
- 543 Kleiner, M., Brainard, D., & Pelli, D. (2007). What's new in Psychtoolbox-3? *Perception, 36,*
544 1–16.
- 545 Köhler, M. H. A., Demarchi, G., & Weisz, N. (in press). Cochlear activity in silent cue-target
546 intervals shows a theta-rhythmic pattern and is correlated to attentional alpha and theta
547 modulations. *BMC Biology*.
- 548 Kontsevich, L. L., & Tyler, C. W. (1999). Bayesian adaptive estimation of psychometric slope

- 549 and threshold. *Vision Research*, 39(16), 2729–2737.
- 550 [https://doi.org/10.1016/S0042-6989\(98\)00285-5](https://doi.org/10.1016/S0042-6989(98)00285-5)
- 551 Litovsky, R. Y., Goupell, M. J., Kan, A., & Landsberger, D. M. (2017). Use of Research
552 Interfaces for Psychophysical Studies With Cochlear-Implant Users. *Trends in Hearing*,
553 21, 2331216517736464. <https://doi.org/10.1177/2331216517736464>
- 554 Loizou, P. C., Hu, Y., Litovsky, R., Yu, G., Peters, R., Lake, J., & Roland, P. (2009). Speech
555 recognition by bilateral cochlear implant users in a cocktail-party setting. *The Journal of*
556 *the Acoustical Society of America*, 125(1), 372–383. <https://doi.org/10.1121/1.3036175>
- 557 Lopez-Poveda, E. A., Eustaquio-Martín, A., Stohl, J. S., Wolford, R. D., Schatzer, R., & Wilson,
558 B. S. (2016). A Binaural Cochlear Implant Sound Coding Strategy Inspired by the
559 Contralateral Medial Olivocochlear Reflex. *Ear and Hearing*, 37(3), e138.
560 <https://doi.org/10.1097/AUD.0000000000000273>
- 561 Maison, S., Micheyl, C., & Collet, L. (2001). Influence of focused auditory attention on cochlear
562 activity in humans. *Psychophysiology*, 38(1), 35–40.
563 <https://doi.org/10.1111/1469-8986.3810035>
- 564 Maris, E., & Oostenveld, R. (2007). Nonparametric statistical testing of EEG- and MEG-data.
565 *Journal of Neuroscience Methods*, 164(1), 177–190.
566 <https://doi.org/10.1016/j.jneumeth.2007.03.024>
- 567 Mazaheri, A., van Schouwenburg, M. R., Dimitrijevic, A., Denys, D., Cools, R., & Jensen, O.
568 (2014). Region-specific modulations in oscillatory alpha activity serve to facilitate
569 processing in the visual and auditory modalities. *NeuroImage*, 87, 356–362.
570 <https://doi.org/10.1016/j.neuroimage.2013.10.052>
- 571 Mc Laughlin, M., Lu, T., Dimitrijevic, A., & Zeng, F. (2012). Towards a Closed-Loop Cochlear
572 Implant System: Application of Embedded Monitoring of Peripheral and Central Neural

- 573 Activity. *IEEE Transactions on Neural Systems and Rehabilitation Engineering*, 20(4),
574 443–454. <https://doi.org/10.1109/TNSRE.2012.2186982>
- 575 Miller, C. A., Brown, C. J., Abbas, P. J., & Chi, S.-L. (2008). The clinical application of potentials
576 evoked from the peripheral auditory system. *Hearing Research*, 242(1), 184–197.
577 <https://doi.org/10.1016/j.heares.2008.04.005>
- 578 Müller, N., & Weisz, N. (2012). Lateralized Auditory Cortical Alpha Band Activity and
579 Interregional Connectivity Pattern Reflect Anticipation of Target Sounds. *Cerebral*
580 *Cortex*, 22(7), 1604–1613. <https://doi.org/10.1093/cercor/bhr232>
- 581 Nelissen, N., Stokes, M., Nobre, A. C., & Rushworth, M. F. S. (2013). Frontal and Parietal
582 Cortical Interactions with Distributed Visual Representations during Selective Attention
583 and Action Selection. *Journal of Neuroscience*, 33(42), 16443–16458.
584 <https://doi.org/10.1523/JNEUROSCI.2625-13.2013>
- 585 O'Brien, F., & Cousineau, D. (2014). Representing Error bars in within-subject designs in typical
586 software packages. *The Quantitative Methods for Psychology*, 10(1), 56–67.
587 <https://doi.org/10.20982/tqmp.10.1.p056>
- 588 Oostenveld, R., Fries, P., Maris, E., & Schoffelen, J.-M. (2010). FieldTrip: Open Source Software
589 for Advanced Analysis of MEG, EEG, and Invasive Electrophysiological Data.
590 *Computational Intelligence and Neuroscience*, 2011, 156869.
591 <https://doi.org/10.1155/2011/156869>
- 592 Pedregosa, F., Varoquaux, G., Gramfort, A., Michel, V., Thirion, B., Grisel, O., Blondel, M.,
593 Prettenhofer, P., Weiss, R., Dubourg, V., Vanderplas, J., Passos, A., Cournapeau, D.,
594 Brucher, M., Perrot, M., & Duchesnay, É. (2011). Scikit-learn: Machine Learning in
595 Python. *Journal of Machine Learning Research*, 12(85), 2825–2830.
- 596 Pelli, D. G. (1997). The VideoToolbox software for visual psychophysics: Transforming numbers

- 597 into movies. *Spatial Vision*, 10(4), 437–442. <https://doi.org/10.1163/156856897X00366>
- 598 Posner, M. I. (1980). Orienting of Attention. *Quarterly Journal of Experimental Psychology*,
- 599 32(1), 3–25. <https://doi.org/10.1080/00335558008248231>
- 600 Prins, N., & Kingdom, F. A. A. (2018). Applying the Model-Comparison Approach to Test
- 601 Specific Research Hypotheses in Psychophysical Research Using the Palamedes
- 602 Toolbox. *Frontiers in Psychology*, 9. <https://doi.org/10.3389/fpsyg.2018.01250>
- 603 Ramekers, D., Versnel, H., Strahl, S. B., Smeets, E. M., Klis, S. F. L., & Grolman, W. (2014).
- 604 Auditory-Nerve Responses to Varied Inter-Phase Gap and Phase Duration of the Electric
- 605 Pulse Stimulus as Predictors for Neuronal Degeneration. *Journal of the Association for*
- 606 *Research in Otolaryngology*, 15(2), 187–202. <https://doi.org/10.1007/s10162-013-0440-x>
- 607 Salo, E., Salmela, V., Salmi, J., Numminen, J., & Alho, K. (2017). Brain activity associated with
- 608 selective attention, divided attention and distraction. *Brain Research*, 1664, 25–36.
- 609 <https://doi.org/10.1016/j.brainres.2017.03.021>
- 610 Sanchez, G., Lecaigard, F., Otman, A., Maby, E., & Mattout, J. (2016). Active SAmpling
- 611 Protocol (ASAP) to Optimize Individual Neurocognitive Hypothesis Testing: A
- 612 BCI-Inspired Dynamic Experimental Design. *Frontiers in Human Neuroscience*, 10.
- 613 <https://doi.org/10.3389/fnhum.2016.00347>
- 614 Sauseng, P., Klimesch, W., Stadler, W., Schabus, M., Doppelmayr, M., Hanslmayr, S., Gruber,
- 615 W. R., & Birbaumer, N. (2005). A shift of visual spatial attention is selectively associated
- 616 with human EEG alpha activity. *European Journal of Neuroscience*, 22(11), 2917–2926.
- 617 <https://doi.org/10.1111/j.1460-9568.2005.04482.x>
- 618 Stypulkowski, P. H., & van den Honert, C. (1984). Physiological properties of the electrically
- 619 stimulated auditory nerve. I. Compound action potential recordings. *Hearing Research*,
- 620 14(3), 205–223. [https://doi.org/10.1016/0378-5955\(84\)90051-0](https://doi.org/10.1016/0378-5955(84)90051-0)

- 621 Suga, N. (2008). Role of corticofugal feedback in hearing. *Journal of Comparative Physiology A*,
622 194(2), 169–183. <https://doi.org/10.1007/s00359-007-0274-2>
- 623 Tejani, V. D., Abbas, P. J., Brown, C. J., & Woo, J. (2019). An improved method of obtaining
624 electrocochleography recordings from Nucleus Hybrid cochlear implant users. *Hearing*
625 *Research*, 373, 113–120. <https://doi.org/10.1016/j.heares.2019.01.002>
- 626 Terreros, G., & Delano, P. H. (2015). Corticofugal modulation of peripheral auditory responses.
627 *Frontiers in Systems Neuroscience*, 9. <https://doi.org/10.3389/fnsys.2015.00134>
- 628 Vallat, R. (2018). Pingouin: Statistics in Python. *Journal of Open Source Software*, 3(31), 1026.
629 <https://doi.org/10.21105/joss.01026>
- 630 Warr, W. B., & Guinan, J. J. (1979). Efferent innervation of the organ of corti: Two separate
631 systems. *Brain Research*, 173(1), 152–155.
632 [https://doi.org/10.1016/0006-8993\(79\)91104-1](https://doi.org/10.1016/0006-8993(79)91104-1)
- 633 Weise, A., Hartmann, T., Schröger, E., Weisz, N., & Ruhnau, P. (2016). Cross-modal distractors
634 modulate oscillatory alpha power: The neural basis of impaired task performance.
635 *Psychophysiology*, 53(11), 1651–1659. <https://doi.org/10.1111/psyp.12733>
- 636 Weisz, N., Hartmann, T., Müller, N., & Obleser, J. (2011). Alpha Rhythms in Audition: Cognitive
637 and Clinical Perspectives. *Frontiers in Psychology*, 2.
638 <https://doi.org/10.3389/fpsyg.2011.00073>
- 639 Weisz, N., Müller, N., Jatzev, S., & Bertrand, O. (2014). Oscillatory Alpha Modulations in Right
640 Auditory Regions Reflect the Validity of Acoustic Cues in an Auditory Spatial Attention
641 Task. *Cerebral Cortex*, 24(10), 2579–2590. <https://doi.org/10.1093/cercor/bht113>
- 642 Winer, J. A. (2006). Decoding the auditory corticofugal systems. *Hearing Research*, 212(1), 1–8.
643 <https://doi.org/10.1016/j.heares.2005.06.014>
- 644 Wittekindt, A., Kaiser, J., & Abel, C. (2014). Attentional Modulation of the Inner Ear: A Combined

645 Otoacoustic Emission and EEG Study. *Journal of Neuroscience*, 34(30), 9995–10002.

646 <https://doi.org/10.1523/JNEUROSCI.4861-13.2014>

647 Woolgar, A., Williams, M. A., & Rich, A. N. (2015). Attention enhances multi-voxel

648 representation of novel objects in frontal, parietal and visual cortices. *NeuroImage*, 109,

649 429–437. <https://doi.org/10.1016/j.neuroimage.2014.12.083>

650 Supplemental Information

651 Methods S1: Details on electrically evoked compound action potentials (ECAPs)

652 ECAPs were biphasic pulses (anodal polarity of the first pulse phase) with a 40 μ s phase
653 duration and an 147 μ s interpulse interval. In each participant, the first (i.e. most apical)
654 electrode was used for stimulation and the second for recording. Phase amplitudes and amount
655 of ECAPs measured in each participant were defined between the minimum amplitude given by
656 the electrical hearing threshold and the maximum amplitude given by the maximum loudness of
657 the standard tone (phase amplitude: in steps of 9.45 current units (CU); amount: in steps of
658 one).

Age	Date(s) of implantation	Deafness onset	Reason(s)	CI model(s)	Side (used)	Residual hearing
53	Unknown	Unknown	Unknown	Unknown	Left	No
51	Unknown	Unknown	Unknown	Unknown	Both (left)	No
44	02/2018	Postlingual	Unknown	RONDO 2	Right	Yes
37	04/2018	Postlingual	Stroke	RONDO 2	Right	Yes
52	10/2015, 12/2016	Postlingual	Sudden deafness	SONNET	Both (left)	No
42	01/2018, 01/2019	Postlingual	Perinatal complications	RONDO 2	Both (right)	No
56	01/2020	Postlingual	Hearing loss in higher frequencies	SONNET 2	Right	Yes
38	07/2011, 08/2020	Postlingual	Sudden deafness (left), middle ear inflammation (right)	SONNET 2	Both (left)	Yes
64	04/2019	Postlingual	Unknown	RONDO 2	Left	Yes
57	06/2018, 06/2019	Postlingual	Age-related hearing loss	SONNET 2 (left),	Both (right)	No

				SONNET (right)		
74	12/2002, 08/2012	Postlingual	Otitis	SONNET 2	Both (left)	No
78	01/2020	Postlingual	Age-related hearing loss	SONNET 2	Left	No
57	08/2014	Postlingual	Sudden deafness	RONDO 2	Right	Yes
70	09/2017	Postlingual	Sudden deafness	SONNET	Right	No
52	06/2014	Postlingual	Age-related hearing loss	SONNET	Left	Yes
55	09/2014, 09/2016	Prelingual	Congenital deafness	SONNET	Both (left)	No

659 **Table S1.** *Overview of CI subjects.* Age (in years) is at the time of the experiment session. In the first two
660 participants, only the age and data of the used side was collected.